Antigen Receptor–induced Activation and Cytoskeletal Rearrangement Are Impaired in Wiskott-Aldrich Syndrome Protein–deficient Lymphocytes

By Jinyi Zhang,*‡§§§ Amro Shehabeldin,*‡§§§ Luis A.G. da Cruz,*‡§§§ Jeffrey Butler,‖‡‡ Ally-Khan Somani,*‡§§§ Mary McGavin,*‡§§§ Ivona Kozieradzki,‡¶** Antonio O. dos Santos,‡¶** Andras Nagy,§§§ Sergio Grinstein,‖‡‡ Josef M. Penninger,‡¶** and Katherine A. Siminovitch*‡§§§

*From the *Department of Medicine, the ‡Department of Immunology, the §Department of Medical Genetics and Microbiology, the ‖Department of Biochemistry, and the ¶Department of Medical Biophysics, University of Toronto, Ontario, Canada M5G 1X5; the **Amgen Institute, Ontario Cancer Institute, Toronto, Ontario, Canada M5G 2C1; the ‡‡Division of Cell Biology, Research Institute, Hospital for Sick Children; and the §§Samuel Lunenfeld Research Institute, Mount Sinai Hospital, Toronto, Ontario, Canada M5G 1X5*

Summary

The Wiskott-Aldrich syndrome protein (WASp) has been implicated in modulation of lymphocyte activation and cytoskeletal reorganization. To address the mechanisms whereby WASp subserves such functions, we have examined WASp roles in lymphocyte development and activation using mice carrying a *WAS* null allele ($WAS^{-/-}$). Enumeration of hemopoietic cells in these animals revealed total numbers of thymocytes, peripheral B and T lymphocytes, and platelets to be significantly diminished relative to wild-type mice. In the thymus, this abnormality was associated with impaired progression from the $CD44^{-}CD25^{+}$ to the $CD44^{-}CD25^{-}$ stage of differentiation. WASp-deficient thymocytes and T cells also exhibited impaired proliferation and interleukin (IL)-2 production in response to T cell antigen receptor (TCR) stimulation, but proliferated normally in response to phorbol ester/ionomycin. This defect in TCR signaling was associated with a reduction in TCR-evoked upregulation of the early activation marker CD69 and in TCR-triggered apoptosis. While induction of TCR-ζ, ZAP70, and total protein tyrosine phosphorylation as well as mitogen-activated protein kinase (MAPK) and stress-activated protein/c-Jun NH_2-terminal kinase (SAPK/JNK) activation appeared normal in TCR-stimulated $WAS^{-/-}$ cells, TCR-evoked increases in intracellular calcium concentration were decreased in WASp-deficient relative to wild-type cells. $WAS^{-/-}$ lymphocytes also manifested a marked reduction in actin polymerization and both antigen receptor capping and endocytosis after TCR stimulation, whereas $WAS^{-/-}$ neutrophils exhibited reduced phagocytic activity. Together, these results provide evidence of roles for WASp in driving lymphocyte development, as well as in the translation of antigen receptor stimulation to proliferative or apoptotic responses, cytokine production, and cytoskeletal rearrangement. The data also reveal a role for WASp in modulating endocytosis and phagocytosis and, accordingly, suggest that the immune deficit conferred by WASp deficiency reflects the disruption of a broad range of cellular behaviors.

Key words: immunodeficiency • Wiskott-Aldrich syndrome protein • antigen receptor signaling • cytoskeletal rearrangement • lymphocyte activation

The Wiskott-Aldrich syndrome (WAS)[1] is an X-linked immune deficiency syndrome classically characterized by the triad of eczema, impaired cellular and humoral immunity, and thrombocytopenia (1, 2). A multiplicity of hemopoietic cell defects have been described among the

J. Zhang, A. Shehabeldin, and L.A.G. da Cruz contributed equally to this work.

[1]*Abbreviations used in this paper:* 7-AAD, 7-amino-actinomycin D; BCR, B cell antigen receptor; ERK, extracellular signal regulatory kinase; ES, embryonic stem; JNK, c-Jun NH_2-terminal kinase; MAPK, mitogen-activated protein kinase; MBP, myelin basic protein; NF-AT, nuclear factor of activated T cells; RAG, recombination activating gene; SAPK, stress-activated protein kinase; sIg, surface Ig; WAS, Wiskott-Aldrich syndrome; WASp, WAS protein.

affected boys, but the most characteristic include impairment in T cell functions such as delayed hypersensitivity and response to allogeneic and mitogenic stimuli, as well as a marked reduction in platelet number, size, and response to agonist stimulation (3–8). These abnormalities have, in turn, been shown to be associated with a spectrum of biochemical defects, most notably including impaired transduction of early activation signals through the antigen receptors on B and T lymphocytes and through the thrombin receptors on platelets (8–12). In addition, WAS patient lymphocytes and platelets manifest cytoskeletal abnormalities, as evidenced in lymphocytes by reduced numbers of surface microvilli projections and an aberrant pattern of actin reorganization after cell stimulation (12, 13); in platelets by altered cell size, shape, and filamentous (F)-actin content (5, 11); and in monocytes by decreased chemotaxis and lack of polarization in response to chemoattractants (14, 15). In view of these observations, WAS has long been considered to reflect the sequela of a protein deficit that disrupts signaling pathways coupling extracellular stimuli to both cytoskeletal rearrangement and nuclear response. Data from X-inactivation studies have revealed the WAS defect to be expressed early in hemopoietic ontogeny (16, 17), and this finding, together with the immunophenotypic characteristics of WAS lymphocytes (18), the functional similarities between WAS B cells and neonatal, immature B cells (19), and the altered *O*-glycosylation profile observed in WAS lymphocyte glycoproteins (20–22), suggest that the WAS phenotype reflects impaired lymphocyte maturation as well as activation and structure.

The product of the WAS gene, WASp, has now been identified (23), and available data concerning the structural and biochemical properties of this cytosolic, hematopoietic-restricted protein are consistent with the hypothesized role for WASp in the regulation of cellular activation and cytoskeletal arrangement (23–25). For example, the protein contains COOH-terminally located regions of homology with the cytoskeletal proteins cofilin and verprolin (26, 27) as well as a cdc42/Rac interactive binding motif that has been shown to mediate WASp binding to the activated form of cdc42 (28). This latter Rho family GTPase has been implicated in the actin reorganization induced by fibroblast stimulation (29) and also in the polarization of the T cell cytoskeleton towards APCs (30). WASp has also been shown to colocalize with actin in T cells and megakaryocytes (31) and to be required for actin remodeling in some hemopoietic lineages (32). Similarly, the yeast WASp homologue, LAS17/Bee1, has been implicated in assembly of the cortical actin cytoskeleton (33); the WASp homologue, N-WASp, has been shown to participate in actin depolymerization and filopodium formation (34); and the WASp-related WASp family Verprolin homologous (WAVE) protein appears to be required for the coupling of Rac to actin rearrangements involved in membrane ruffling (35). These observations, together with data demonstrating that suppressor of cAR (SCAR1), another WASp family protein, as well as WASp itself interact with the actin-related protein (Arp2/3) complex and are involved in formation of platelet-derived growth factor–induced lamellipodia (36, 37), indicate a pivotal role for WASp in regulating actin organization and the cytoskeletal rearrangements induced by external stimuli.

In addition to its interactions with cdc42 and cytoskeletal components, WASp also contains a putative pleckstrin homology domain at its NH_2 terminus (38) and a proline-rich region which has been shown to interact with Nck, Fyn, and several other Src homology 3 (SH3) domain–containing proteins implicated in intracellular activation cascades (39–44). These properties of WASp suggest that the functions subserved by this protein include not only cytoskeletal modification, but also intracellular transduction of activating signals. This latter contention is consistent with data demonstrating that antigen receptor–induced proliferation is impaired in WAS patients (9, 10) as well as in WASp-deficient mice (45). At present, however, the mechanisms whereby WASp influences cell activation and structural arrangement are poorly understood. In this context, we have derived mice carrying a *WAS* null allele and examined the effects of WASp deficiency on lymphocyte development and response to antigen receptor stimulation. Analyses of these $WAS^{-/-}$ animals has provided definitive evidence of a critical role for WASp in coupling antigen receptor engagement to both receptor capping and endocytosis and to the signaling cascades that evoke proliferation, IL-2 production, and apoptosis. The data also reveal an important role for WASp in driving the development/expansion of mature peripheral T and B cells and in promoting the progression of immature thymocytes from the double-negative to the $CD4^+CD8^+$ double-positive stage. However, investigation of the signaling pathways downstream of TCR engagement indicate that early activation events such as tyrosine phosphorylation of ZAP70, TCR-ζ, and other cellular proteins, as well as activation of the mitogen-activated protein kinase (MAPK) and the stress-activated protein/c-Jun NH_2-terminal kinase (SAPK/JNK), are unaffected by WASp deficiency. Together, these observations identify WASp as a regulator of lymphocyte ontogeny, cytoskeletal structure, and activation and suggest that WASp effects on lymphocyte behavior are realized through modulation of the cytoskeletal processes governing antigen receptor rearrangement and terminal activation events such as proliferation and cytokine production.

Materials and Methods

Reagents. Antibodies used for these studies included the following: FITC-conjugated Ly9.1, anti–Thy 1.2, anti-CD8, anti-Fas, anti-IgM, anti-CD4, anti-CD5, and anti-IgD; PE-conjugated anti-CD4, anti-CD3ε, anti-CD44, anti-CD43, anti-CD23, and anti–IL-2 and anti-B220; biotin-conjugated anti–TCR-α/β, anti-IgD, anti-CD19, and anti-CD25; allophycocyanin-conjugated anti–TCR-α/β, anti-CD3, anti-CD4, anti-CD8, anti-B220, anti-CD40, and anti-IgM antibodies and Cy5-conjugated streptavidin, all from PharMingen; and anti–extracellular signal regulatory kinase (ERK)1 and anti-ERK2 antibodies from Santa Cruz, anti–TCR-ζ and anti-ZAP70 antibodies supplied by Drs. Larry Samelson (National Institutes of Health, Bethesda, MD) and André Veillette (McGill

Cancer Centre, Montreal, Quebec, Canada), respectively; and antiphospho-SAPK/JNK and anti-SAPK/JNK antibodies (reactive against all SAPK/JNK isoforms) from New England Biolabs. Texas red–conjugated streptavidin was purchased from GIBCO BRL. Monoclonal hamster anti–mouse CD3ε was produced by the 145-2C11 hybridoma (provided by Dr. R. Miller, Ontario Cancer Institute) and purified from the supernatant by protein G chromatography; polyclonal rabbit anti-WASp antibody was derived by immunization with a polylysine-conjugated peptide corresponding to a putative nuclear localization signal within the *WAS* cDNA; anti–murine β-actin mAb, PMA, ionomycin, and murine recombinant IL-2 were purchased from Sigma Chemical Co.; rabbit anti–hamster and anti–mouse IgG antibodies and FITC-conjugated streptavidin were purchased from Jackson ImmunoResearch Laboratories. Murine recombinant IL-4 was obtained from PharMingen, [^{3}H]thymidine from Dupont/NEN, 7-aminoactinomycin D (7-AAD) from Calbiochem, Indo-1 from Molecular Probes, myelin basic protein (MBP) from Upstate Biotechnology, Inc., and an IL-2 ELISA kit from Genzyme. Brefeldin A was a gift from Dr. R. Miller.

Generation of WASp-deficient Mice. A *WAS* gene targeting vector was derived by subcloning a 3.3-kb segment of the *WAS* gene encompassing ~2 kb of the 5′ flanking sequence upstream of the initiation codon through exon 4 of the gene into the Ssc8387I site of the pPNT expression cassette (46) and a 3.4-kb fragment encompassing the XbaI site in exon 11 through to a BamHI site within intron 11 into the pPNT XbaI-BamHI sites. Embryonic stem (ES) cells from the male-derived R1 ES cell line (129/Sv) were electroporated with this targeting vector and selected with neomycin and gancyclovir (47). Surviving clones were screened for homologous recombination at the *WAS* locus by PCR using the following primer pair: 5′-GTGAAGGATAACCCTCAGAAGTCC-3′ (forward primer, S1, derived from sequences within exon 2 of the *WAS* gene) and 5′-CGGAGCAGAATCTAGATGGCAGAGT-3′ (reverse primer, S2, representing sequences in the 3′ region downstream from exon 12 of the *WAS* gene) (see Fig. 1 A). Targeted clones were verified by Southern blotting with a probe derived from a 450-bp segment external to the 5′ region of homology (see Fig. 1 B). Two independently derived $WAS^{-/-}$ clones were then either aggregated with CD1 eight cell stage embryos or microinjected into 3.5-d recombinase activating gene 2–deficient ($RAG\text{-}2^{-/-}$) blastocysts (48), and the aggregates or blastocysts were then implanted into pseudopregnant foster mothers.

WAS genotypes of the chimeric progeny were confirmed using a PCR assay including the forward primer (G1; 5′-ACTGAAGGCTCTTTACTATTGCT-3′), derived from a sequence within the neomycin resistance gene, and a reverse primer (G2; 5′-ACTGAAGCCTCTTTACTATTGCT-3′), corresponding to a sequence within exon 11 of the *WAS* gene. Chimeric male mice carrying the mutation in the germline were bred to the C57BL/6 background by backcrossing over six generations.

Flow Cytometry Analysis. Cells were resuspended in immunofluorescence staining buffer (PBS containing 1% BSA and 0.05% NaN_3) and incubated with the appropriate fluorochrome-conjugated antibodies for 30 min at 4°C. For three- and four-color staining, Texas red– or Cy5-conjugated streptavidin was used after staining with biotin-conjugated antibodies. Stained cells were analyzed using a FACScan™ with CELLQuest™ software (Becton Dickinson). For detection of expression of the early activation marker CD69, thymocytes (2×10^6 cells/ml) were cultured with medium alone, with plate-bound anti-CD3 antibody (10 μg/ml), or with plate-bound anti-CD3 plus anti-CD28 antibodies (10 and 0.2 μg/ml, respectively) for 24 h. Cells were stained with FITC-conjugated anti-CD8, PE-conjugated anti-CD4, and biotinylated anti-CD69 antibodies followed by Cy5-conjugated streptavidin. Expression of CD69 was measured on gated $CD4^+$ $CD8^+$ thymocytes.

Cell Stimulation. For analysis of cell proliferation, single cell suspensions were prepared from thymi, lymph nodes, and spleen of age-matched $WAS^{-/-}$ and $WAS^{+/+}$ (C57BL/6) mice bred at the Samuel Lunenfeld Research Institute, and the cells were then subjected to erythrocyte lysis in ammonium chloride buffer. Thymocytes and lymph node cells were cultured in 96-well flat-bottomed microtiter plates (2×10^6 cells/ml) for 48 h in culture medium alone or in the presence of either plate-bound (0–25 μg/ml) or soluble (2 μg/ml) anti-CD3ε antibody with or without anti-CD28 antibody (0.2 μg/ml) or with soluble anti-CD3 antibody plus PMA (1 μg/ml and 5 ng/ml, respectively), Con A (1 μg/ml) or PMA plus ionomycin (5 μg/ml and 250 ng/ml, respectively), or soluble anti-CD3 antibody plus IL-2 (1 μg/ml and 50 U/ml, respectively). Splenocytes (2×10^6 cells/ml) were cultured for 48 h with medium alone, LPS (5 μg/ml), IL-4 (2 ng/ml), or IL-4 plus anti-IgM antibody $F(ab')_2$ fragment (1.25 and 5 μg/ml), or anti-CD40 antibody (2 μg/ml). Cultured cells were pulsed with [^{3}H]thymidine (1 μCi/well) for 16 h before terminating the incubation. Incorporated radioactivity was measured using an automated β scintillation counter. Alternatively, for biochemical assays, 4×10^7 thymocytes or lymph node T cells were resuspended in 100 μl 2% FCS–containing RPMI and incubated for 30 min at 4°C in the presence or absence of biotin-conjugated anti-CD3 antibody (25 μg/ml). After removal of unbound antibody, the cells were resuspended at a concentration of 2×10^8 cells/ml, warmed to 37°C for 1 min, and incubated for varying periods with 10 μg/ml streptavidin.

Evaluation of IL-2 Production. To evaluate IL-2 secretion, supernatants were collected from unstimulated and TCR-stimulated cells and the amount of IL-2 was quantified by ELISA (Genzyme). Numbers of IL-2–producing cells were assayed by incubating stimulated and unstimulated lymph node T cells (2×10^6) in 24-well plates precoated with anti-CD3 antibody (5 μg/ml) with or without addition of soluble anti-CD28 antibody (4 μg/ml) and in the presence or absence of Brefeldin A (5 μM) at 37°C for 8 h. Cells were harvested, washed with immunofluorescence buffer, and labeled with an FITC-conjugated anti-CD4 antibody. Cells were then washed again and incubated for 15 min in 150 μl of 4% paraformaldehyde at room temperature. Cells were then washed, permeabilized, and labeled by 2-h incubation with a PE-conjugated anti–IL-2 antibody in 100 μl of 0.1% saponin–containing immunofluorescence buffer. Cells were washed twice with permeabilization buffer, resuspended in immunofluorescence buffer, and analyzed by flow cytometry.

Immunoblotting, Immunoprecipitation, and MAPK Assay. Splenocytes and thymocytes (2×10^6 cells) from $WAS^{+/+}$ and $WAS^{-/-}$ mice were lysed in buffer containing 50 mM Tris, pH 7.5, 150 mM NaCl, 1% Triton X-100, 1 mM PMSF, and 1 μg/ml each of leupeptin, pepstatin, and aprotinin as protease inhibitors. After 15 min incubation in cold lysis buffer, unlysed cells were removed by centrifugation and the lysates were then boiled in the presence of 6× reducing sample buffer, electrophoresed through 10% SDS-polyacrylamide, and transferred to nitrocellulose (Schleicher & Schuell). The filters were incubated at 4°C for at least 1 h in TBST solution (150 mM NaCl, 10 mM Tris-HCl, pH 7.4, 0.05% Tween 20) plus 3% gelatin. Filters were then incubated for 2 h at room temperature with anti-WASp antibody (1 μg/ml) in TBST, followed by the addition of goat anti–mouse antiserum la-

beled with peroxidase (Amersham Pharmacia Biotech) and horseradish peroxidase conjugate (Bio-Rad Laboratories). The blot was stripped and reprobed with an anti–β-actin antibody in order to assess loading. For immunoprecipitation, lysates prepared from unstimulated or TCR-stimulated thymocytes or lymph node T cells (4×10^7) were precleared by incubating an equal amount (100–250 μg) lysate protein with protein A–Sepharose (Amersham Pharmacia Biotech) for 1 h at 4°C and for an additional 1 h with 40 μl rabbit preimmune sera. Lysates were then incubated for 3 h at 4°C with specific antibody or rabbit preimmune serum and 25 μl packed protein A–Sepharose beads, and the immune complexes were then collected by centrifugation, washed four times in lysis buffer, and resuspended in SDS sample buffer for immunoblotting analyses. Alternatively, ERK1/ERK2 immune complexes immunoprecipitated using a mixture of anti-ERK1 and anti-ERK2 antibodies were washed in MAPK buffer (5 mM Hepes, pH 7.4, 10 mM $MgCl_2$, 100 mM $NaVO_4$) and resuspended in 50 μl reaction buffer (30 mM Tris-HCl, pH 8.0, 20 mM $MgCl_2$, 2 mM $MnCl_2$ containing 5 μg MBP [Upstate Biotechnology], 1 mM cold ATP, and 10 μCi [γ-^{32}P]ATP [Dupont/NEN]). After 15 min incubation at 30°C, reactions were terminated by addition of 12 μl 6× SDS-PAGE loading buffer, and the samples were boiled, electrophoresed through 12% polyacrylamide gels, and transferred to nitrocellulose. The phosphorylated MBP bands were visualized by autoradiography, and ERK1 and ERK2 expression levels were determined by anti-ERK2 immunoblotting analysis.

Measurement of Ca^{2+} Influx. Thymocytes and lymph node T cells (5×10^6 cells/ml) were labeled with Indo-1 (5 μM) and incubated at 37°C in the dark for 30 min. Cells were washed, resuspended in RPMI containing 2% FBS and 10 mM Hepes, pH 7.4, and incubated with biotinylated anti-TCR antibody (5 μg/ml) for 15 min at 4°C. After washing, the cells were resuspended in RPMI buffer at a concentration of 10^7 cells/ml and stimulated with 5 μg/ml of streptavidin. Calcium levels were detected by flow cytometric analysis of Indo-1 violet-blue fluorescence ratio (49).

Induction of Apoptosis. Freshly isolated thymocytes were plated at a density of 2×10^6 cells/ml in 96-well tissue culture plates precoated with either anti-CD3 antibody (20 μg/well), anti-CD3 plus anti-CD28 (each 20 μg/well), anti-Fas antibody (0.1, 1, or 5 μg/ml), or PMA plus ionomycin (10 and 500 ng/ml, respectively). After 24 h, the cells were harvested, washed with PBS, and stained with FITC-conjugated anti-CD4, PE-conjugated anti-CD8, and 7-AAD (10 μg/ml) for 30 min on ice (50). After three washes, the cells were analyzed using the Becton Dickinson FACScan™ and CELLQuest™ software.

Capping and Endocytosis of T and B Cell Antigen Receptors. 10^6 cells were incubated with 1 μg/ml of biotinylated anti-TCR (thymus) or 1 μg/ml of biotinylated anti–mouse IgD (spleen), for 30 min on ice. After washing, cells were labeled for 30 min on ice with 1 μg/ml streptavidin-FITC. Cells were washed and resuspended in 100 μl of RPMI and incubated at 37°C for 5 min. The cells were pelleted in a microcentrifuge for 15 s and then fixed for 15 min in 2% paraformaldehyde. After washing twice in 0.5% BSA–containing PBS, the cells were cytospun onto slides and mounted with SlowFade Light (Molecular Probes). The cells were visualized with a confocal fluorescence microscope (MRC-600; Bio-Rad Laboratories). The average percentage of capped cells was obtained from 10 microscope fields per sample (100–200 cells/field).

Internalization of the TCR was assayed by incubating 10^6 lymph node T cells with anti-CD3 antibody (1 μg/ml) for 30 min on ice. After washing, cells were incubated with biotinylated goat anti–hamster antibody (2 μg/ml) for 30 min at 4°C and then warmed at 37°C. Aliquots were removed at varying time points thereafter, transferred to ice, and the reaction was stopped by addition of 0.1% NaN_3. Cells were then stained with FITC-conjugated streptavidin, fixed for 15 min in 4% paraformaldehyde, and washed before analysis by flow cytometry.

Actin Polymerization Assay. Thymocytes were incubated with anti-CD3ε (1 μg/ml) for 30 min on ice. After washing, the primary antibodies were cross-linked using goat anti–hamster Ig (1 μg/ml) for 5 min. The control cells were incubated only with the cross-linking antibody. Activation was terminated by addition of 4% paraformaldehyde. After fixation, cells were incubated with FITC-conjugated phalloidin (Sigma Chemical Co.) for 30 min, washed three times in PBS, and analyzed using a FACSCalibur™.

Phagocytosis. Long bones (humerus, femur, tibia) were removed from selected mice, and the ends were then clipped and flushed using a 27-gauge needle and ice-cold HBSS. Clumps of marrow were then broken up by repeated pipetting, and the cells were spun at 500 *g* at 4°C for 5 min, resuspended in HBSS in a 15-ml polypropylene tube, and underlaid with a discontinuous Percoll gradient (52, 65, and 75% Percoll solution). Cells were then centrifuged at 1,500 *g* for 30 min at 4°C, and the neutrophil-enriched fraction (at the interface of the 65 and 75% gradients) was harvested, diluted with an equal volume of HBSS, and spun down in a microfuge for 10 s. These cells were resuspended in 1 ml of RPMI and counted using a Coulter counter. To evaluate phagocytosis, cells were mixed with opsonized zymosan (10 particles/cell) and lucifer yellow at 0.5 mg/ml, pelleted in a microfuge tube, and then incubated for 5 min at 37°C. Cells were then washed three times in ice-cold PBS, and the number of cells with lucifer yellow–containing phagosomes was counted using a fluorescence microscope.

Results and Discussion

WASp Deficiency Engenders a Defect in Lymphoid Ontogeny. To derive ES cells carrying a disruption of the *WAS* gene, a targeting construct was developed in which a 3.5-kb segment encompassing intron 4 to exon 11 of the *WAS* gene was substituted with the pPNT expression vector. This vector was then introduced into R1 ES cells, and two clones carrying a WAS mutant allele were then aggregated with CD1 eight cell embryos. Once germline transmission of the targeted allele was confirmed by PCR and Southern analysis (Fig. 1, A and B), the *WAS* mutation was bred into the C57BL/6 background. The two $WAS^{-/-}$ ES cell clones were also injected into $RAG^{-/-}$ blastocysts so as to derive $WAS^{-/-}RAG^{-/-}$ chimeric mice which were used in addition to the $WAS^{-/-}$ mice for some studies of lymphocyte function. As illustrated by immunoblotting analysis, male mice carrying the *WAS* mutant allele showed no WASp expression in either thymic or splenic cells (Fig. 1 C) despite the presence of surface (s)Ig^+ B cells and mature $CD4^+$ $CD8^-$ and $CD4^-CD8^+$ T cells (Fig. 1 D).

Although lymphoid cells were present in the $WAS^{-/-}$ mice, an analysis of cell numbers in these animals revealed lymphocyte cellularity to be reduced in all lymphoid organs examined. A reduction in lymphoid cell number was most evident in the thymus, where the number of thymocytes was about one quarter of that observed in wild-type mice

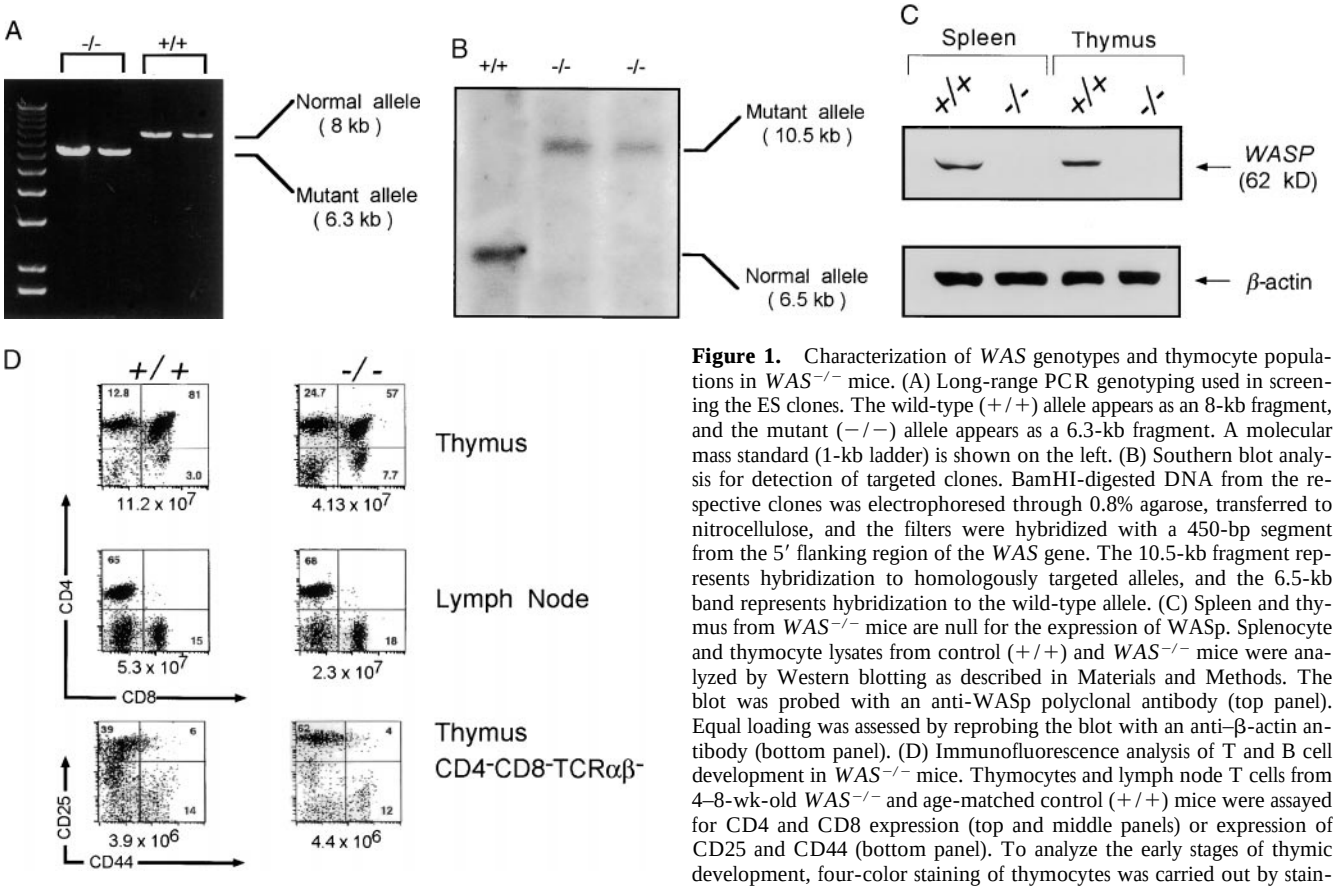

Figure 1. Characterization of *WAS* genotypes and thymocyte populations in $WAS^{-/-}$ mice. (A) Long-range PCR genotyping used in screening the ES clones. The wild-type (+/+) allele appears as an 8-kb fragment, and the mutant (−/−) allele appears as a 6.3-kb fragment. A molecular mass standard (1-kb ladder) is shown on the left. (B) Southern blot analysis for detection of targeted clones. BamHI-digested DNA from the respective clones was electrophoresed through 0.8% agarose, transferred to nitrocellulose, and the filters were hybridized with a 450-bp segment from the 5′ flanking region of the *WAS* gene. The 10.5-kb fragment represents hybridization to homologously targeted alleles, and the 6.5-kb band represents hybridization to the wild-type allele. (C) Spleen and thymus from $WAS^{-/-}$ mice are null for the expression of WASp. Splenocyte and thymocyte lysates from control (+/+) and $WAS^{-/-}$ mice were analyzed by Western blotting as described in Materials and Methods. The blot was probed with an anti-WASp polyclonal antibody (top panel). Equal loading was assessed by reprobing the blot with an anti–β-actin antibody (bottom panel). (D) Immunofluorescence analysis of T and B cell development in $WAS^{-/-}$ mice. Thymocytes and lymph node T cells from 4–8-wk-old $WAS^{-/-}$ and age-matched control (+/+) mice were assayed for CD4 and CD8 expression (top and middle panels) or expression of CD25 and CD44 (bottom panel). To analyze the early stages of thymic development, four-color staining of thymocytes was carried out by staining the cells with a cocktail containing allophycocyanin-labeled anti-CD3, anti-CD4, anti-CD8, anti–TCR-α/β, and anti-B220 antibodies, and subsequently with FITC-Ly9.1, biotinylated anti-CD25 (detected with Texas red–conjugated streptavidin), and PE-labeled anti-CD44. Fluorescence signals were evaluated using Becton Dickson FACScan™ and CELLQuest™ software and were gated to display CD25 versus CD44 on Ly-9.1$^+$ (ES-derived) CD4, CD8, CD3 triple-negative cells (bottom panel). Numbers in the quadrants indicate percentages of different cell populations, while numbers below each panel indicate total number of thymic cells. Data shown are representative of four independent experiments.

(Table I). Reduced thymic cellularity appeared to reflect a decrease in the total and relative numbers of $CD4^+CD8^+$ double-positive thymocytes, an abnormality which, in turn, was associated with relative increases in the numbers of double-negative $CD4^-CD8^-$ and single-positive $CD4^+$ $CD8^-$ and $CD4^-CD8^+$ cells (Fig. 1 D). Although this defect was not detected in a previous analysis of WASp-deficient mice (45), the current findings are consistent with several lines of evidence revealing lymphocyte maturation to be altered in WAS patients (17, 18, 22). To further examine this maturation defect, the $CD4^-CD8^-$ double-negative precursors, identified by virtue of negative staining for CD4, CD8, B220, TCR-α/β, and TCR-γ/δ, were evaluated for expression of the maturation markers CD25 and CD44. These latter markers have been previously shown to identify four double-negative thymocyte subsets, $CD44^+CD25^-$, $CD44^+CD25^+$, $CD44^-CD25^+$, and $CD44^-$ $CD25^-$, which demarcate progressive stages of thymocyte maturation (51). As shown in Fig. 1 D (lower panel), among these four double-negative subsets, the $CD44^-CD25^+$ population was relatively increased and the $CD44^-CD25^-$ population relatively decreased in the $WAS^{-/-}$ compared with wild-type mice. Thus the reduction in total thymocyte numbers observed in the absence of WASp appears to reflect impaired progression of the $CD44^-CD25^+$ to the $CD44^-CD25^-$ stage and by extension, reduced transit from the double-negative to the double-positive stage. Interest-

Table I. *Cell Numbers in $WAS^{-/-}$ Mice*

	Total no. of cells ($\times 10^{-6}$) ± SD	
Tissue	+/+	$WAS^{-/-}$
Thymus	116.0 ± 16.6	43.6 ± 12.5
Lymph nodes	49.3 ± 10.0	24.8 ± 2.7
Spleen	47.0 ± 7.8	20.4 ± 2.8
Bone marrow	10.3 ± 1.4	10.0 ± 2.6
Platelets	616.0 ± 65.4	377.8 ± 94.2

Total thymocytes, total mesenteric, axillary and inguinal lymph node T cells, total splenocytes, and bone marrow cells (one femur) from wild-type (+/+; $n = 4$) and $WAS^{-/-}$ ($n = 4$) mice were isolated and counted; blood platelet count (cells/ml) was determined from tail-bled wild-type and $WAS^{-/-}$ mice ($n = 5$).

ingly, this same perturbance in thymocyte maturation has also been detected in animals deficient for the CD45 (52), Lck (53), and Vav (54, 55) signaling effectors, an observation which strongly suggests that this defect reflects diminished signaling, most likely via the pre-TCR (56).

WAS$^{-/-}$ thymocytes were also examined for expression of TCR-α/β, CD3, and the maturation marker CD5, all of which were found to be expressed normally on the mutant thymocytes (data not shown). Similarly, analysis of splenic and bone marrow B cell populations revealed expression of CD43, CD19, CD23, CD86, CD25, B220, sIgM, and sIgD to be comparable in *WAS*$^{-/-}$ and wild-type mice (data not shown). However, for thymocytes, total numbers of peripheral CD4^{+}CD8^{-} and CD4^{-}CD8^{+} T cells and peripheral B220^{+}sIgM^{+} B cells were reduced by ~50% in the *WAS*$^{-/-}$ chimeric compared with wild-type animals (Table I). Together, these data indicate lymphopoiesis to be impaired, albeit not arrested, in the context of WASp deficiency. WASp effects on lymphoid ontogeny appear to be predominantly realized in the thymic compartment at the double-negative stage of thymocyte differentiation, and it may be for this reason, as well as sensitivity of this defect to strain background (54), that impaired thymic ontogeny was not detected in an independently derived *WAS*$^{-/-}$ mouse (45). Importantly, however, in the latter mice, as well as in some WAS patients (6), significant reductions of peripheral T lymphocyte number have been observed. Thus, the available evidence strongly suggests a role for WASp in driving the maturation and/or expansion of T and possibly mature B cell populations. Whether this latter role is subserved by WASp modulation of the proliferation/expansion and/or survival of lymphoid precursors remains to be determined. Alternatively, the reduction in lymphocyte number observed in the *WAS*$^{-/-}$ mice might reflect perturbation in the transit of immature precursors from the bone marrow to other lymphoid organs.

In addition to lymphocytes, platelets were also found to be reduced in the periphery of *WAS*$^{-/-}$ mice. As shown in Table I and consistent with the detection of thrombocytopenia in virtually all WAS patients, platelet number was reduced by ~40% in the *WAS*$^{-/-}$ relative to wild-type mice. At present, the basis for this finding remains unclear, with preliminary data revealing that platelet survival is normal in these animals (data not shown). The physiologic significance of this defect is also unclear, as the *WAS*$^{-/-}$ mice, in contrast to classical WAS patients, show no overt signs of a hemorrhagic diathesis.

Antigen Receptor–induced Activation Is Impaired in WASp-deficient Lymphocytes. In view of previous data suggesting that antigen receptor–evoked lymphocyte activation is impaired in WAS patients (9, 10, 12), thymocytes and peripheral B and T lymphocytes from the *WAS*$^{-/-}$ chimeras were next studied with respect to their responses to antigen receptor ligation. The results of these analyses revealed that anti-CD3 antibody–evoked proliferation was markedly reduced in *WAS*$^{-/-}$ relative to *WAS*$^{+/+}$ thymocytes (Fig. 2 A) at all anti-CD3 antibody concentrations tested (data not shown). Similarly, Con A stimulation elicited significantly less proliferation in *WAS*$^{-/-}$ thymocytes than wild-type cells. By contrast, the mutant cells proliferated normally in response to PMA and ionomycin, a maneuver which triggers proliferation in the absence of antigen receptor engagement. In addition, anti-CD3 as well as anti-CD3 plus anti-CD28 antibody–induced upregulation of the CD69 early activation marker (57, 58) were markedly diminished in the mutant cells (Fig. 2 D).

Similar to *WAS*$^{-/-}$ thymocytes, WASp-deficient peripheral T cells were also observed to have reduced proliferative responses to anti-CD3 antibody, but a normal response to PMA and ionomycin (Fig. 2 B). However, *WAS*$^{-/-}$ peripheral T cells also responded, albeit less than wild-type cells, to anti-CD3 antibody stimulation combined with PMA treatment, whereas addition of CD28 could partially restore proliferation of these cells (Fig. 2 B, left panel). Anti-CD3–induced proliferative responses of the WASp-deficient cells were also restored to almost normal levels by the addition of IL-2 (Fig. 2 B, right panel). To investigate the basis for this latter finding, anti-CD3–induced production of IL-2 was also evaluated in the *WAS*$^{-/-}$ T cells. As shown in Fig. 2 E, wild-type T cells secreted only a small amount of IL-2 after anti-CD3 antibody treatment, but dramatically increased their IL-2 production in conjunction with anti-CD28 antibody–mediated costimulation. However, in the *WAS*$^{-/-}$ cells, IL-2 production was not only negligible after anti-CD3 antibody stimulation, but also increased by much less (50%) in these cells than in wild-type cells after CD28 costimulation (Fig. 2 E). This defect in the induction of IL-2 does not reflect impairment of IL-2 secretion, as an evaluation of IL-2 production based on intracellular staining of T cells stimulated with anti-CD3/anti-CD28 antibodies in the presence of the secretion blocker Brefeldin A (59, 60) revealed the numbers of IL-2–staining cells to be ~50% less in the *WAS*$^{-/-}$ relative to wild-type cell cultures (Fig. 2 E). By contrast, in the absence of Brefeldin A, IL-2 accumulation was not detected in the mutant or wild-type cells, indicating the IL-2 secretion pathway to be intact in the context of WASp deficiency. Thus, these observations indicate that WASp effects on TCR signaling are modulated by costimulatory signals and also suggest that the T cell proliferative defect conferred by WASp deficiency is due, at least in part, to a defect in IL-2 production. Taken together, these data confirm the participation of WASp in the transduction of activation signals via the TCR and suggest that the effects of WASp on TCR-mediated activation are most profound in immature T cells and may be tempered by concomitant activation signals delivered via CD28, IL-2, and possibly other stimulatory receptors. The data also identify potential functional differences between the T cells of the WASp-deficient mice studied here and those of WAS patients in whom anti-CD3–induced proliferative responses appear to be only partially restored by exogenous IL-2 (10). While further studies are required to determine whether this discrepancy reflects the use of transformed WAS patient cell lines, the current data provide definitive evidence of a role for WASp in promoting the coupling of TCR stimulation to T cell activation and to the IL-2 production integral to normal T cell mitogenesis.

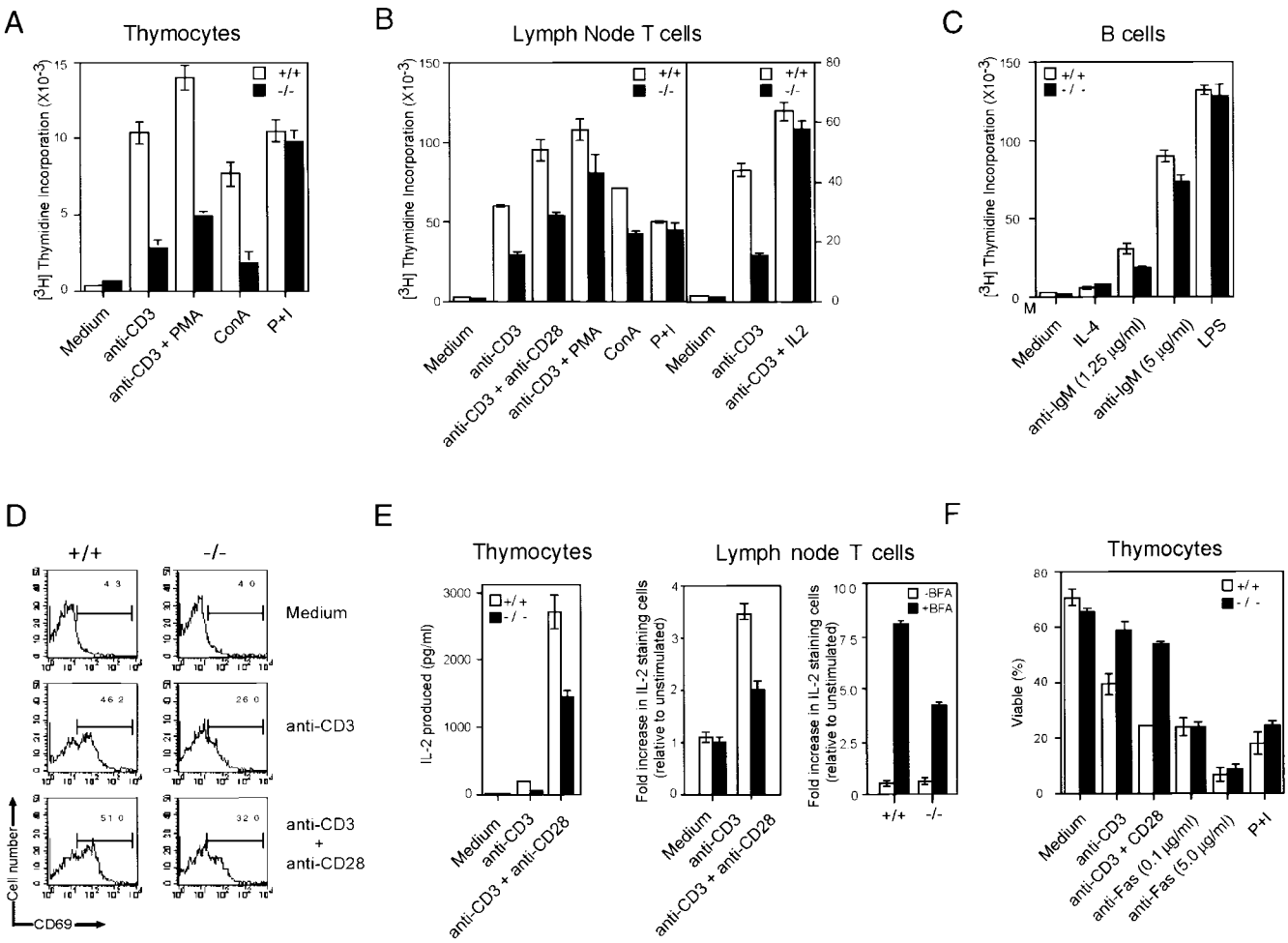

Figure 2. Effects of WASp deficiency on antigen receptor–evoked proliferation, IL-2 production, and apoptosis. (A) Freshly isolated T and B lymphocytes from the thymi (A), lymph nodes (B), and spleens (C) of 4–8-wk-old $WAS^{-/-}$ mice (−/−) or age-matched control mice (+/+) were cultured for 48 h with the following stimuli. For thymocytes: anti-CD3 antibody (2 μg/ml), anti-CD3 antibody plus PMA (5 ng/ml), Con A (1 μg/ml), or PMA and ionomycin (P+I, 250 ng/ml); for lymph node T cells: anti-CD3 antibody (1 μg/ml), anti-CD3 antibody plus anti-CD28 antibody (0.2 μg/ml), anti-CD3 antibody plus PMA (5 ng/ml), Con A (1 μg/ml), PMA and ionomycin (P+I, 250 ng/ml), or anti-CD3 antibody plus 50 U/ml IL-2; for splenic cells: IL-4 (2 ng/ml), anti-IgM (1.25 or 5 μg/ml), or LPS (5 μg/ml). Proliferative responses were determined after a 16-h pulse with [3H]thymidine. Values represent means (±SEM) of triplicate cultures and are representative of one of four independent experiments. (D) Flow cytometric analysis of the expression of the early activation marker CD69 upon treatment of thymocytes with either medium alone (top), anti-CD3 antibody (middle), or anti-CD3 plus anti-CD28 antibodies (bottom). (E) IL-2 production by $WAS^{-/-}$ and $WAS^{+/+}$ thymocytes stimulated for 48 h with anti-CD3 antibody (2 μg/ml) or anti-CD3 plus anti-CD28 antibody (2 and 0.2 μg/ml, respectively) was evaluated by ELISA of culture supernatants (left panel). Alternatively, lymph node T cells were cultured for 8 h with medium alone or with anti-CD3 (5 μg/ml) or anti-CD3/anti-CD28 (5 μg/ml/4 μg/ml) antibodies, stained with FITC-conjugated anti-CD4 antibody followed by permeabilization and staining with PE-conjugated anti–IL-2 antibody, and analyzed by flow cytometry (middle panel). Results are expressed as the fold increase in numbers of IL-2–stained $CD4^+$ cells in stimulated relative to unstimulated wild-type cells and represent means (±SEM) of triplicate cultures. Intracellular staining of $WAS^{-/-}$ and $WAS^{+/+}$ lymph node cells stimulated with anti-CD3/anti-CD28 in the presence or absence of Brefeldin A was also evaluated as above (right panel). Values represent means (±SEM) of triplicate cultures. (F) Thymocytes from $WAS^{-/-}$ and control $WAS^{+/+}$ mice were activated by incubation with either medium alone or with plate-bound anti-CD3 antibody (20 μg/well), anti-CD3 plus anti-CD28 antibodies (each 20 μg/well), anti-Fas (0.1 or 5 μg/ml) antibody, or with PMA plus ionomycin (P+I, 10 and 500 ng/ml, respectively) for 24 h, after which the cells were stained with 7-AAD (10 μg/ml) and with FITC-conjugated anti-CD4 and PE-conjugated anti-CD8 and analyzed by flow cytometry. Histograms indicate the percentage of viable $CD4^+CD8^+$ cells. Values represent means (±SEM) of triplicate cultures and are representative of four independent experiments.

In contrast to thymocytes and peripheral T cells, WASp-deficient splenic B cells showed only a marginal reduction in response to antigen receptor ligation, a finding that was not altered by varying the concentrations of anti-Ig antibody (Fig. 2 C). As observed in $WAS^{-/-}$ T cells, this mild reduction in responsiveness of the WASp-deficient B cells to mitogenic stimulus appears to be antigen receptor specific, as these cells proliferated normally in response to LPS, IL-4 (Fig. 2 C), and the combination of IL-4 with anti-CD40 antibody (data not shown). Thus, WASp deficiency appears to be associated with impairment in T cell and to a much lesser extent, B cell antigen receptor (BCR) signaling. While a defect in BCR signaling was not reported in a previous study of WASp-deficient mice (45), the current findings are consistent with data indicating that antigen receptor–evoked B cell proliferative responses are impaired

in patients with classical WAS (9). However, it is currently unclear whether the divergent effects of WASp deficiency on TCR versus BCR signaling reflect differences in the biochemical requirements required for signal delivery by the respective receptors or the capacity of another effector, such as N-WASp, to adequately subserve WASp functions in B, but not T cells.

In view of these data identifying a role for WASp in coupling antigen receptor engagement to lymphocyte proliferation, the possibility that this protein also modulates antigen receptor capacity to activate cell death cascades was also investigated. Specifically, $WAS^{-/-}$ and wild-type double-positive thymocytes were cultured for 24 h in the presence of anti-CD3 antibody alone or combined with anti-CD28 antibody, and the viability and rate of cellular apoptosis were then evaluated in $CD4^+CD8^+$ cells by immunofluorescence analysis of 7-AAD staining. As shown in Fig. 2 F, results of this analysis revealed that viability of the anti-CD3–stimulated $WAS^{-/-}$ $CD4^+CD8^+$ cells was ~35% greater than that of wild-type cells. This difference was even more marked in the context of anti-CD3/anti-CD28 stimulation. By contrast, cell viability after anti-Fas antibody or PMA/ionomycin treatment was similar in the mutant and wild-type cells. Therefore, these data indicate that WASp specifically modulates the apoptotic as well as mitogenic signaling cascades evoked by TCR engagement. At present, the physiologic significance of these findings remains unclear, although the involvement of WASp in TCR-mediated apoptosis implies a potential role for this protein in facilitating negative selection events in the thymus, a possibility which might be etiologically relevant to the autoimmune phenomena frequently expressed by WAS patients (6).

Antigen Receptor–induced Tyrosine Phosphorylation and Activation of MAPK and SAPK/JNK Appear Normal in WASp-deficient T Cells. To elucidate the biochemical basis for the T cell functional defects conferred by WASp deficiency, $WAS^{-/-}$ T cells were evaluated with respect to the signaling events elicited by TCR engagement. As indicated by the antiphosphotyrosine immunoblots shown in Fig. 3, A and B, the levels of TCR-ζ, ZAP70, and total cellular protein tyrosine phosphorylation detected in resting and TCR-stimulated $WAS^{-/-}$ thymocytes and peripheral T cells were

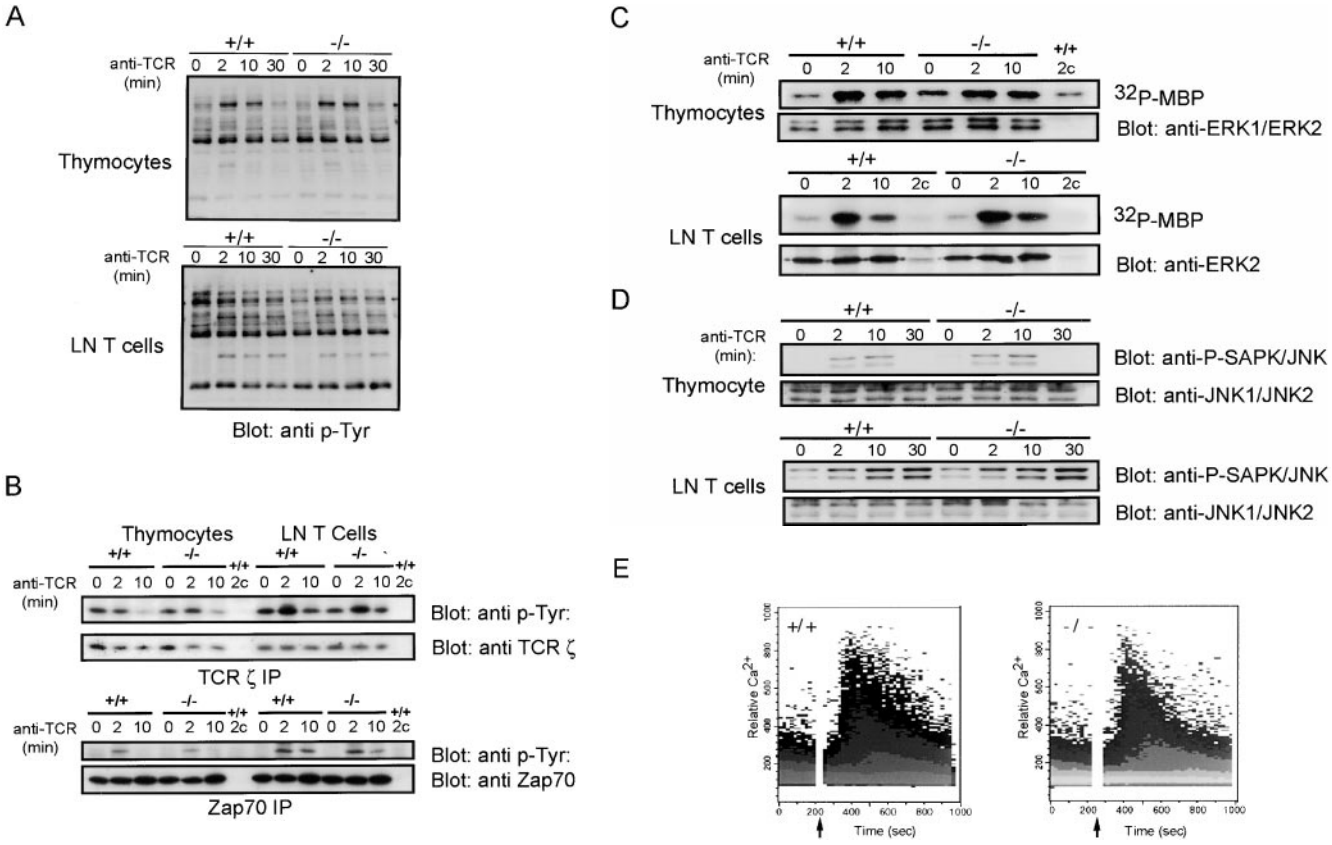

Figure 3. Effects of WASp deficiency on TCR signaling. $WAS^{-/-}$ or $WAS^{+/+}$ thymocytes or lymph node T cells were stimulated with biotinylated anti-TCR antibody (10 μg/ml) followed by streptavidin cross-linking (10 μg/ml) for the indicated times. Lysates were prepared as in Materials and Methods, and the lysate proteins were either (A) resolved over SDS-PAGE and subjected to antiphosphotyrosine immunoblotting analysis; (B) subjected to immunoprecipitation with anti–TCR-ζ (top panel) or anti-ZAP70 (bottom panel) antibodies as well as control rabbit IgG(c) and subsequent sequential immunoblotting with antiphosphotyrosine (anti p-Tyr) and anti–TCR-ζ or anti-ZAP70 antibodies, respectively; (C) immunoprecipitated with anti-ERK1 and anti-ERK2 antibodies as well as control IgG(c), and the immune complexes were evaluated for ability to phosphorylate MBP by SDS-PAGE and autoradiography (upper panel) and for amount of ERK1 and ERK2 by immunoblotting analysis (lower panel); or (D) resolved over SDS-PAGE and subjected to sequential immunoblotting analysis with antiphospho-SAPK/JNK (pSAPK/JNK) and anti-SAPK/JNK (JNK1 and JNK2) antibodies. (E) Flow cytometric analysis of Ca^{2+} influx after stimulation of thymocytes with anti–TCR-α/β antibody. Arrows indicate addition of cross-linking streptavidin.

essentially identical to those observed in similarly treated wild-type cells. Along similar lines, TCR-evoked increases in MAPK activation and in phosphorylation, and presumably activation of SAPK/JNK were comparable (Fig. 3, C and D). By contrast, the increase in intracellular calcium levels induced by TCR ligation was less sustained in the $WAS^{-/-}$ compared with wild-type cells, with intracellular calcium concentrations 20 and 25% reduced in the $WAS^{-/-}$ relative to wild-type cells at the 600- and 700-s time points, respectively (Fig. 3 E). At present, it is unclear whether this quantitative difference in intracellular calcium mobilization observed in wild-type compared with $WAS^{-/-}$ cells translates to a sufficiently significant perturbance of other downstream signaling events, such as NF-AT translocation to the nucleus, so as to account for the very significant impairment in TCR-induced IL-2 expression by the mutant cells.

Antigen Receptor–induced Actin Polymerization, Capping, and Endocytosis Are Defective in WASp-deficient Lymphocytes. As WASp has also been implicated by many lines of evidence in the regulation of cytoskeletal architecture, the relevance of WASp to lymphocyte cytoskeletal rearrangements induced by antigen receptor engagement was also investigated. To this end, $WAS^{-/-}$ lymphocytes were studied with respect to the induction of antigen receptor capping, a phenomenon that requires de novo actin polymerization and microfilament rearrangement. As indicated in Fig. 4 A and illustrated by the representative micrograph (Fig. 4 B), a defect in ligand-induced capping was detected in $WAS^{-/-}$

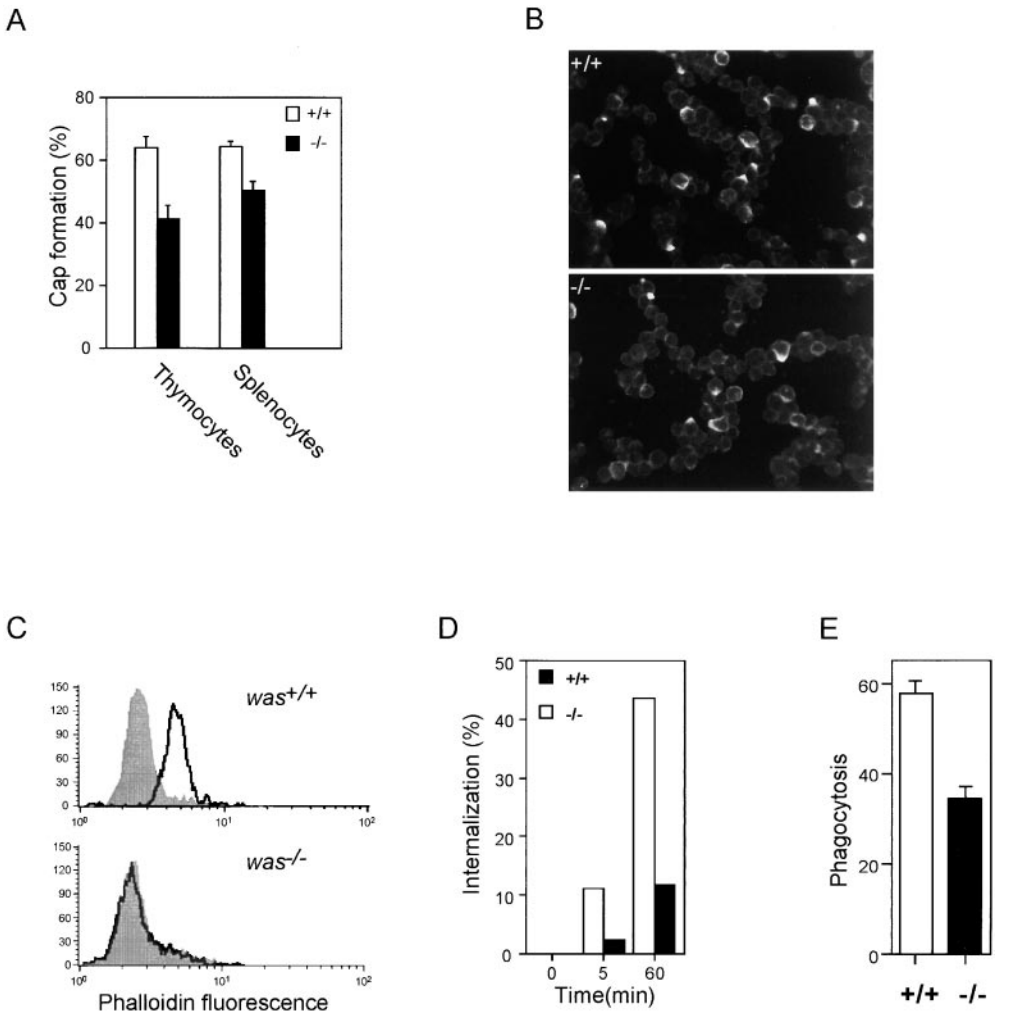

Figure 4. Analysis of lymphocyte cap formation, actin polymerization, and endocytosis and neutrophil phagocytosis in $WAS^{-/-}$ mice. (A) Percentages (±SD) of $WAS^{+/+}$ and $WAS^{-/-}$ thymocytes and splenic B cells showing antigen receptor clustering after antigen receptor ligation. Peripheral lymph node T cells and splenic cells from $WAS^{-/-}$ and wild-type (+/+) mice were incubated with soluble biotinylated anti-TCR antibody (1 μg/ml) or with 1 μg/ml biotinylated anti–mouse IgD antibody, respectively, followed by FITC-conjugated streptavidin and then fixed with 2% paraformaldehyde as described in Materials and Methods. Capped cells were then visualized by fluorescence confocal microscopy, and the percentage of capped cells was determined by scoring cells from 10 microscope fields per sample (100–200 cells/field). (B) Fluorescence confocal micrograph (original magnification: ×126) showing TCR capping of anti-TCR–stimulated thymocytes (as above) from $WAS^{-/-}$ (bottom) and wild-type (top) mice. (C) Impairment of actin polymerization in $WAS^{-/-}$ mice. Thymocytes from $WAS^{-/-}$ and $WAS^{+/+}$ mice were isolated and stimulated with anti-CD3ε antibody (1 μg/ml) for 30 min on ice, followed by cross-linking with a secondary antibody (outlined histograms) or alternatively, treated with the secondary antibody alone (filled histograms). Cells were fixed with 4% paraformaldehyde, and F-actin content was quantitated by flow cytometric analysis of FITC-phalloidin–stained cells. One result representative of three independent experiments is shown. (D) TCR internalization in $WAS^{-/-}$ T cells. Lymph node T cells from $WAS^{-/-}$ and wild-type mice were incubated for 30 min on ice with anti-CD3 antibody (1 μg/ml) and then washed and incubated for an additional 30 min on ice with biotinylated goat anti–hamster antibody (2 μg/ml). Cells were then warmed to 37°C, and aliquots were removed at 5 and 60 min, mixed with 0.1% NaN_3 on ice, and stained with FITC-conjugated streptavidin. Cells were then fixed for 15 min in 4% paraformaldehyde, and surface TCR expression was analyzed by flow cytometry. (E) Phagocytic activity of bone marrow neutrophils from $WAS^{-/-}$ mice. Neutrophils were purified from $WAS^{-/-}$ and wild-type bone marrow as described in Materials and Methods and then incubated for 5 min at 37°C with opsonized zymosan and lucifer yellow. Cells were then washed, and the percentage of lucifer yellow–containing phagosomes was evaluated by fluorescence microscopy. The percent phagocytosis was calculated from the total number of cells with lucifer yellow–stained phagosomes relative to the total number of cells in six to eight high-power fields. Values represent the mean ± SEM of five independent experiments.

thymocytes, the number of these cells showing T cell antigen receptor clustering to be ~40% less than that of wild-type thymocytes. As is consistent with a defect, albeit mild in BCR-induced proliferation, anti-Ig–mediated capping of the BCR was also impaired in the context of WASp deficiency. In addition, immunofluorescence analysis of anti-CD3–treated phalloidin-labeled $WAS^{-/-}$ thymocytes, an assay that selectively detects expression of polymerized F-actin, revealed that antigen receptor–mediated actin polymerization was markedly reduced in $WAS^{-/-}$ thymocytes (Fig. 4 C) and lymph node T cells (data not shown). Together, these data demonstrate a requirement for WASp in the regulation of cytoskeletal rearrangement in response to antigen receptor engagement.

In addition to patch and cap formation, internalization of antigen receptors after their engagement appears to require cytoskeletal rearrangement, as endocytosis of these receptors is abrogated by cytoskeleton-disrupting agents such as dihydrocytochalasin B (61). In view of this observation, together with data from our lab (Siminovitch, K., unpublished observations) and another (62) revealing the capacity of WASp and the Las17/Beel yeast WASp homologue, respectively, to interact with proteins implicated in endocytosis, the possibility that WASp plays a role in ligand-triggered TCR endocytosis was investigated by assaying the levels of biotinylated TCR present on $WAS^{-/-}$ T cells at varying times after cell stimulation. As illustrated in Fig. 4 C, the results of this analysis revealed the rate of TCR endocytosis to be markedly reduced in the context of WASp deficiency, with 50% of the receptors internalized in wild-type cells, but only 10% internalized in $WAS^{-/-}$ cells at 1 h after stimulation. Therefore, these results suggest the involvement of WASp in the process of receptor endocytosis. At present, the level at which the endocytic pathway is disrupted by WASp deficiency remains unclear. However, this defect may also impact on the properties of nonlymphoid cells, as opsonized zymosan particle internalization was also found to be significantly reduced in $WAS^{-/-}$ compared with wild-type neutrophils (Fig. 4 E). Together, these data raise the possibility that the altered endocytosis of the TCR and/or other receptors and consequent changes in levels of surface receptor expression impact on a broad range of immune cellular functions, including not only cell activation, but also maintenance of cell polarity, antigen presentation, and/or the uptake of extracellular nutrients and microorganisms.

In summary, the current data reveal that transduction of TCR-evoked proliferation, apoptosis, and actin polymerization–inducing signals are impaired in $WAS^{-/-}$ T cells. WASp deficiency also engenders a defect in thymocyte maturation, by impairment of the progression of $CD4^-$ $CD8^-$ progenitors from the $CD44^-CD25^+$ to a $CD44^-$ $CD25^-$ stage. This developmental defect may reflect diminished signaling capacity of the pre-TCR in the absence of WASp, as has been previously proposed in relation to the similar, albeit more severe, maturational defect detected in Lck-deficient thymocytes (53). Similarly, the reduction in peripheral T cell numbers conferred by WASp deficiency may reflect not only impaired thymopoiesis, but also diminished proliferative/expansion potential consequent to defective transduction of TCR mitogenic signals. As is consistent with the immunologic abnormalities described in WAS patients, the early stages of B cell ontogeny appear intact and BCR-induced proliferation is only modestly diminished in the context of WASp deficiency. However, the reduction in splenic B cell numbers and in capping capacity of stimulated antigen receptors on $WAS^{-/-}$ B cells implies that the modest diminution in antigen receptor–evoked B cell proliferation is physiologically relevant and may engender impaired expansion of B cells within the peripheral compartment.

Despite the plethora of functional defects detected in $WAS^{-/-}$ T cells and thymocytes, many of the biochemical events involved in signal relay through the TCR (such as tyrosine phosphorylation and MAPK and SAPK/JNK activation) remain intact in these cells. In this context, the $WAS^{-/-}$ cells are strikingly similar to the lymphoid cells of mice genetically rendered deficient for Vav (63–65), a guanine nucleotide exchange factor for the Rho family of GTPases (66, 67). Although the effect of Vav deficiency on B cell ontogeny and function is more prominent than that of WASp deficiency, $Vav^{-/-}$ mice manifest defects in T cell maturation, TCR-evoked proliferation, cytokine production, and actin polymerization that closely resemble those observed in the $WAS^{-/-}$ mice. In addition, as with $WAS^{-/-}$ T cells, $Vav^{-/-}$ T cells show little or no abnormalities with respect to the early activation events induced by TCR ligation. At present, the biochemical basis whereby both the structural (receptor clustering and actin polymerization) and physiologic (proliferation and cytokine production) sequelae of TCR ligation are disrupted by WASp or Vav deficiency remains unclear. However, a relationship between these facets of T cell activation has become increasingly well recognized and is strongly supported by recent data indicating a pivotal role for cytoskeletal rearrangement in reorienting the T cell–APC interface so as to create a framework for the incorporation of signaling molecules into supramolecular activation clusters (SMACs) that amplify signal delivery (68, 69). Taken together with the T cell defects observed in $WAS^{-/-}$ mice, these observations suggest that while TCR activation signals can be initiated in the absence of cytoskeletal-driven events such as receptor clustering, signal delivery in this context is insufficient to achieve optimal activation and cytokine production. Thus, by virtue of its capacity to interact with both cdc42 and the Arp2/3 complex, WASp may act to promote the spatial rearrangements required for SMAC formation and thereby facilitate the juxtaposition of activated antigen receptors and signaling molecules that is required for efficient transduction of activation signals. Accordingly, the defective actin polymerization and TCR clustering engendered by WASp deficiency would predictably translate to signaling of insufficient amplitude and/or duration for optimal activation and cytokine production. This hypothesis is supported by preliminary data revealing that T cell microtubule organizing center (MTOC) polarization toward the T cell–APC contact site is reduced in stimulated $WAS^{-/-}$ T cells (Burkhardt, J., and K. Siminovitch, data not shown) and, if

correct, might explain the disparate effects of WASp deficiency on B cell versus T cell activation, the latter of which appears more highly dependent on proper actin filament assembly (70, 71). In view of data indicating CD28–B7 interaction to be both necessary and sufficient for inducing movement of the cortical actin cytoskeleton toward the TCR–ligand interface (68), the capacity of CD28 costimulation to partially normalize TCR-evoked proliferative responses of $WAS^{-/-}$ T cells suggests that WASp effects on cytoskeletal rearrangement may be particularly important for the propagation of TCR-initiated signals evoked in the absence of costimulatory signal. The capacity of WASp to interact with Nck may also be of some relevance to WASp effects on TCR signaling, as the Nck adaptor protein has been shown to promote TCR-mediated NF-AT activation by virtue of an interaction with the Pak1 serine/threonine kinase (40). As Pak1, like WASp, appears to act downstream of cdc42 activation in a JNK-independent fashion, these observations suggest that WASp effects on TCR-evoked IL-2 production may reflect not only WASp modulation of upstream cytoskeletal-mediated TCR rearrangements, but also WASp interactions with both activated cdc42 and Nck. While these hypotheses require further investigation, the current data indicate that mice with WASp-deficient lymphoid cells provide a valuable system for dissecting out the complex structural and biochemical properties of WASp and delineating the molecular events that couple antigen receptor stimulation to cytoskeletal rearrangement and lymphocyte activation.

The authors thank Dr. Gordon Mills for helpful discussions, Denis Bouchard for assistance with immunofluorescence analysis, Marina Gertsenstein for assistance with the ES cell work and aggregations, and Dr. Tak Mak for his generosity in facilitating the genesis of the $WAS^{-/-}$ mice.

This work was supported by grants to K.A. Siminovitch and J.M. Penninger from the Medical Research Council of Canada. K.A. Siminovitch is a Research Scientist of the Arthritis Society of Canada; L.A.G. da Cruz is a recipient of a fellowship from the Fundação para a Ciência e a Tecnologia of Portugal; and A.K. Somani is supported by a Steve Fonyo studentship from the National Cancer Institute of Canada.

Address correspondence to Katherine A. Siminovitch, Mount Sinai Hospital, Rm. 656A, 600 University Ave., Toronto, Ontario, Canada M5G 1X5. Phone: 416-586-4692; Fax: 416-586-8558; E-mail: ksimin@mshri.on.ca

Submitted: 21 July 1999 Revised: 27 August 1999 Accepted: 2 September 1999

References

1. Aldrich, R.A., A.G. Steinberg, and D.C. Campbell. 1954. Pedigree demonstrating a sex-linked recessive condition characterized by draining ears, eczematoid dermatitis and bloody diarrhea. *Paediatrics*. 13:133–138.
2. Cooper, M.D., H.P. Chase, J.T. Lowman, W. Krivit, and R.A. Good. 1968. The Wiskott-Aldrich syndrome: an immunologic deficiency disease involving the afferent limb of immunity. *Am. J. Med*. 44:499–513.
3. Ochs, H.D., S.J. Slichter, L.A. Harker, W.E. von Behrens, R.A. Clark, and R.J. Wedgwood. 1980. The Wiskott-Aldrich syndrome: studies of lymphocytes, granulocytes, and platelets. *Blood*. 55:243–252.
4. Spitler, L.E., A.S. Levin, D.P. Stites, H.H. Fudenberg, and H.H. Huber. 1975. The Wiskott-Aldrich syndrome. Immunologic studies in nine patients and selected family members. *Cell. Immunol*. 19:201–218.
5. Grottum, K.A., T. Hovig, H. Holmsen, A.F. Abrahamson, M. Jeremic, and M. Seip. 1969. Wiskott-Aldrich syndrome: qualitative platelet defects and short platelet survival. *Br. J. Haematol*. 17:373–388.
6. Sullivan, K.E., C.A. Mullen, R.M. Blaese, and J.A. Winkelstein. 1994. A multiinstitutional survey of the Wiskott-Aldrich syndrome. *J. Pediatr*. 125:876–885.
7. Greer, W.L., and K.A. Siminovitch. 1994. Molecular characterization of the X-linked immunodeficiency diseases. *Clin. Immunol. News*. 14:17–25.
8. Marone, G., F. Albini, L. di Martino, S. Quattrin, S. Poto, and M. Condorelli. 1986. The Wiskott-Aldrich syndrome: studies of platelets, basophils and polymorphonuclear leucocytes. *Br. J. Haematol*. 62:737–745.
9. Simon, H.-U., G.B. Mills, S. Hashimoto, and K.A. Siminovitch. 1992. Evidence for defective transmembrane signaling in B cells from patients with Wiskott-Aldrich syndrome. *J. Clin. Invest*. 90:1376–1405.
10. Molina, I.J., J. Sancho, C. Terhorst, F.S. Rosen, and E. Remold-O'Donnell. 1993. T cells of patients with the Wiskott-Aldrich syndrome have a restricted defect in proliferative responses. *J. Immunol*. 151:4383–4390.
11. Semple, J.W., K.A. Siminovitch, M. Mody, Y. Milev, A.H. Lazarus, J.F. Wright, and J. Freedman. 1997. Flow cytometric analysis of platelets from children with the Wiskott-Aldrich syndrome reveals defects in platelet development activation and structure. *Br. J. Haematol*. 97:747–754.
12. Gallego, M.D., M. Santamaria, J. Pena, and I.J. Molina. 1997. Defective actin organization and polymerization of Wiskott-Aldrich T cells in response to CD3-mediated stimulation. *Blood*. 90:3089–3097.
13. Kenney, D., L. Cairns, E. Remold-O'Donnell, J. Peterson, F.S. Rosen, and R. Parkman. 1986. Morphological abnormalities in the lymphocytes of patients with the Wiskott-

Aldrich syndrome. *Blood*. 68:1329–1332.
14. Zicha, D., W.E. Allen, P.M. Brickell, C. McKinnon, G.A. Dunn, G.E. Jones, and A.J. Thrasher. 1998. Chemotaxis of macrophages is abolished in the Wiskott-Aldrich syndrome. *Br. J. Haematol*. 101:659–665.
15. Badolato, R., S. Sozzani, F. Malacarne, S. Bresciani, M. Fiorini, A. Borsatti, A. Albertini, A. Mantovani, A.G. Ugazio, and L.D. Notarangelo. 1998. Monocytes from Wiskott-Aldrich patients display reduced chemotaxis and lack of cell polarization in response to monocyte chemoattractant protein-1 and formyl-methionyl-leucyl-phenylalanine. *J. Immunol*. 161: 1026–1033.
16. Prchal, J.T., A.J. Carroll, J.F. Prchal, W.M. Crist, H.W. Skalka, W.J. Gealy, and A. Mulluh. 1980. Wiskott-Aldrich syndrome: cellular impairments and their implication for carrier detection. *Blood*. 56:1048–1052.
17. Greer, W.L., P.C. Kwong, M. Peacocke, P. Ip, L.A. Rubin, and K.A. Siminovitch. 1989. Y-chromosome inactivation in the Wiskott-Aldrich syndrome: a marker for detection in the carrier state and identification of cell lineages expressing the *WAS* gene defect. *Genomics*. 4:60–67.
18. Morio, T., K. Takase, H. Okawa, M. Oguchi, M. Kanbara, F. Hiruma, K. Yoshino, T. Kaneko, S. Asamura, T. Inoue, et al. 1989. The increase of non-MHC-restricted cytotoxic cells (γ/δ-TCR-bearing T cells or NK cells) and the abnormal differentiation of B cells in Wiskott-Aldrich syndrome. *Clin. Immunol. Immunopathol*. 52:279–290.
19. Golding, B., A.V. Muchmore, and R.M. Blaese. 1984. Newborn and Wiskott-Aldrich patient B cells can be activated by TNP-*Brucella abortus*: evidence that TNP-*Brucella abortus* behaves as a T-independent type I antigen in humans. *J. Immunol*. 133:2966–2971.
20. Greer, W.L., E. Higgins, D.R. Sutherland, A. Novogrodsky, I. Brockhausen, M. Peacocke, L.A. Rubin, M. Baker, J.W. Dennis, and K.A. Siminovitch. 1989. Altered expression of leucocyte sialoglycoprotein in Wiskott-Aldrich syndrome is associated with a specific defect in O-glycosylation. *Biochem. Cell Biol*. 67:503–509.
21. Piller, F., F. Le Deist, K.I. Weinberg, R. Parkman, and M. Fukuda. 1991. Altered *O*-glycan synthesis in lymphocytes from patients with Wiskott-Aldrich syndrome. *J. Exp. Med*. 173:1501–1510.
22. Higgins, E.A., K.A. Siminovitch, D. Zhuang, I. Brockhausen, and J.W. Dennis. 1991. Aberrant O-linked oligosaccharide biosynthesis in lymphocytes and platelets from patients with the Wiskott-Aldrich syndrome. *J. Biol. Chem*. 266:6280–6290.
23. Derry, J.M.J., H.D. Ochs, and U. Francke. 1994. Isolation of a novel gene mutated in Wiskott-Aldrich syndrome. *Cell*. 78: 635–644.
24. Parolini, O., S. Berardelli, E. Riedl, C. Bello-Fernandez, H. Strobl, O. Majdic, and W. Knapp. 1997. Expression of Wiskott-Aldrich syndrome protein (WASp) gene during haemopoietic differentiation. *Blood*. 90:70–75.
25. Stewart, D.M., S. Trieber-Held, C.C. Kurman, F. Facchetti, L.D. Notarangelo, and D.L. Nelson. 1996. Studies of the expression of the Wiskott-Aldrich syndrome protein. *J. Clin. Invest*. 97:2627–2634.
26. Miki, H., and T. Takenawa. 1998. Direct binding of the verprolin-homology domain in N-WASp to "actin" is essential for cytoskeletal reorganization. *Biochem. Biophys. Res. Commun*. 243:73–78.
27. Nishida, E., S. Maekawa, and H. Sakai. 1984. Cofilin, a protein in porcine brain that binds to actin filaments and inhibits their interactions with myosin and tropo-myosin. *Biochemistry*. 23:5307–5313.
28. Aspenström, P., U. Lindberg, and A. Hall. 1995. Two GTPases, Cdc42 and Rac, bind directly to a protein implicated in the immunodeficiency disorder, Wiskott-Aldrich syndrome. *Curr. Biol*. 6:70–75.
29. Nobes, C.D., and A. Hall. 1995. Rho, rac and Cdc42 GTPases regulate the assembly of multimolecular focal complexes associated with actin stress fibers, lamellipodia and filopodia. *Cell*. 81:53–62.
30. Stowers, L., D. Yelon, L.J. Berg, and J. Chant. 1995. Regulation of the polarization of T cells toward antigen-presenting cells by Ras-related GTPase CDC42. *Proc. Natl. Acad. Sci. USA*. 92:5027–5031.
31. Symons, M., J.M.J. Derry, B. Karlak, S. Jiang, V. Lemahieu, F. McCormick, U. Francke, and A. Abo. 1996. Wiskott-Aldrich syndrome protein, a novel effector for the GTPase cdc42Hs, is implicated in actin polymerization. *Cell*. 84: 723–734.
32. Miki, H., S. Nonoyama, Q. Zhu, A. Aruffo, H.D. Ochs, and T. Takenawa. 1997. Tyrosine kinase signaling regulates Wiskott-Aldrich syndrome protein function, which is essential for megakaryocyte differentiation. *Cell Growth Differ*. 8:195–202.
33. Li, R. 1997. Bee1, a yeast protein with homology to Wiskott-Aldrich syndrome protein, is critical for the assembly of cortical actin cytoskeleton. *J. Cell Biol*. 136:649–658.
34. Miki, H., T. Sasaki, Y. Takai, and T. Takenawa. 1998. Induction of filopodium formation by a WASp-related actin-depolymerizing protein N-WASp. *Nature*. 39:93–96.
35. Miki, H., S. Suetsugu, and T. Takenawa. 1998. WAVE, a novel WASP-family protein involved in actin reorganization induced by Rac. *EMBO (Eur. Mol. Biol. Organ.) J*. 17:6932–6941.
36. Bear, J.E., J.F. Rawls, and C.L. Saxe III. 1998. SCAR, a WASp-related protein, isolated as a suppressor of receptor defects in late *Dictyostelium* development. *J. Cell Biol*. 142: 1325–1335.
37. Machesky, L.M., and R.H. Insall. 1998. Scar1 and the related Wiskott-Aldrich syndrome protein, WASP, regulate the actin cytoskeleton through the Arp2/3 complex. *Curr. Biol*. 8:1347–1356.
38. Miki, H., K. Miura, and T. Takenawa. 1996. N-WASP, a novel actin-depolymerization protein, regulates the cortical cytoskeletal rearrangement in a PIP2-dependent manner downstream of tyrosine kinase. *EMBO (Eur. Mol. Biol. Organ.) J*. 15:5326–5335.
39. Rivero-Lezcano, O.M., A. Marcilla, J.H. Sameshima, and K.C. Robbins. 1995. Wiskott-Aldrich syndrome protein physically associates with Nck through Src homology 3 domains. *Mol. Cell. Biol*. 15:5725–5731.
40. Yablonski, D.L., P. Kane, D. Qian, and A. Weiss. 1998. A Nck-Pak1 signaling module is required for T-cell receptor-mediated activation of NF-AT, but not of JNK. *EMBO (Eur. Mol. Biol. Organ.) J*. 17:5647–5657.
41. Bunnel, S.C., P.A. Henry, R. Kolluri, T. Kirchhausen, R.J. Rickles, and L.J. Berg. 1996. Identification of Itk/Tsk Src homology 3 domain ligands. *J. Biol. Chem*. 271:25646–25656.
42. Banin, S., O. Truong, D.R. Katz, M.D. Waterfield, P.M. Brickell, and I. Gout. 1996. Wiskott-Aldrich syndrome protein (WASp) is a binding partner for c-SRC family protein-tyrosine kinases. *Curr. Biol*. 6:981–988.

43. Cory, G.O.C., L. MacCarthy-Morrogh, S. Banin, I. Gout, P.M. Brickell, R.J. Levinsky, C. Kinnon, and R.C. Lovering. 1996. Evidence that the Wiskott-Aldrich syndrome protein may be involved in lymphoid cell signaling pathways. *J. Immunol.* 157:3791–3795.
44. Tinan, P.M., C.J. Soames, L. Wilson, D.L. Nelson, D.M. Stewart, O. Truong, J.S. Hsuan, and S. Kellie. 1996. Identification of regions of the Wiskott-Aldrich syndrome protein responsible for association with selected Src homology 3 domains. *J. Biol. Chem.* 271:26291–26295.
45. Snapper, S.B., F.S. Rosen, E. Mizoguchi, P. Cohen, W. Khan, C.H. Liu, T.L. Hagemann, S.P. Kwan, R. Ferrini, L. Davidson, et al. 1998. Wiskott-Aldrich syndrome protein-deficient mice reveal a role for WASP in T but not B cell activation. *Immunity*. 9:81–91.
46. Tybulewicz, V.L.J., C.E. Crawford, P.K. Jackson, R.T. Bronson, and R.C. Mulligan. 1991. Neonatal lethality and lymphopenia in mice with a homozygous disruption of the c-abl proto-oncogene. *Cell*. 65:1153–1163.
47. Pirity, M., A. Hadjantonakis, and A. Nagy. 1998. Embryonal stem cells, creating transgenic animals. *Methods Cell Biol.* 57: 279–293.
48. Chen, J., R. Lansford, V. Stewart, F. Young, and F. Alt. 1993. RAG-2-deficient blastocyst complementation: an assay of gene function in lymphocyte development. *Proc. Natl. Acad. Sci. USA*. 90:4528–4532.
49. Rabinovitch, P.S., C.H. June, A. Grossmann, and J.A. Ledbetter. 1986. Heterogeneity among T cells in intracellular free calcium responses after mitogen stimulation with PHA or anti-CD3. Simultaneous use of indo-1 and immunofluorescence with flow cytometry. *J. Immunol.* 137:952–961.
50. Barton, K., N. Muthasami, M. Chanyangam, C. Fisher, C. Clendenin, and J.M. Leiden. 1996. Defective thymocyte proliferation and IL-2 production in transgenic mice expressing a dominant-negative form of CREB. *Nature*. 379:81–85.
51. Godfrey, D.I., J. Kennedy, T. Suda, and A. Zlotnik. 1993. A developmental pathway involving four phenotypically and functionally distinct subsets of $CD3^-CD4^-CD8^-$ triple-negative adult mouse thymocytes defined by CD44 and CD25. *J. Immunol.* 150:4244–4252.
52. Byth, K.F., L.A. Conroy, S. Howlett, A.J.H. Smith, J. May, D.R. Alexander, and N. Holmes. 1996. CD45-null transgenic mice reveal a positive regulatory role for CD45 and early thymocyte development, in the selection of $CD4^+$ $CD8^+$ thymocytes and B cell maturation. *J. Exp. Med.* 183: 1707–1718.
53. Levin, S.D., S.J. Anderson, K.A. Forbush, and R.M. Perlmutter. 1993. A dominant-negative transgene defines a role for $p56^{lck}$ in thymocytes. *EMBO (Eur. Mol. Biol. Organ.) J.* 12:1671–1680.
54. Fischer, K.D., Y.Y. Khong, H. Nishina, K. Tedford, L.E. Marengere, I. Kozieradzki, T. Sasaki, M. Starr, G. Chan, S. Gardner, et al. 1998. Vav is a regulator of cytoskeleton reorganization mediated by the T-cell receptor. *Curr. Biol.* 8:554–562.
55. Turner, M., P.J. Mee, A.E. Walters, M.E. Quinn, A.L. Mellor, R. Zamoyska, and V.L. Tybulewicz. 1997. A requirement for the Rho-family GTP exchange factor Vav in positive and negative selection of thymocytes. *Immunity*. 7:451–460.
56. Saint-Ruf, C., K. Ungewiss, M. Groettrap, L. Bruno, J.J. Tehling, and H. von Boehmer. 1994. Analysis and expression of a cloned pre-T receptor gene. *Science*. 266:1208–1212.
57. Swat, W., M. Dessing, H. von Boehmer, and P. Kisielow. 1993. CD69 expression during selection and maturation of $CD4^+CD8^+$ thymocytes. *Eur. J. Immunol.* 23:739–746.
58. Testi, R., J.H. Phillips, and L.L. Lamei. 1989. Leu23 induction as an early marker of functional CD3/T cell antigen receptor triggering. Requirement for receptor cross-linking, prolonged elevation of intracellular $[Ca^{++}]$ and stimulation of protein kinase C. *J. Immunol.* 142:1854–1860.
59. Misumi, Y., Y. Misumi, K. Miki, A. Takatsuki, G. Tamura, and Y. Ikehara. 1986. Novel blockade by brefeldin A of intracellular transport of secretory proteins in cultured rat hepatocytes. *J. Biol. Chem.* 261:11398–11403.
60. Picker, L.J., M.K. Singh, Z. Zdraveski, J.R. Treer, S.L. Waldrop, P.R. Bergstresser, and V.C. Maino. 1995. Direct demonstration of cytokine synthesis heterogeneity among human memory/effector T cells by flow cytometry. *Blood.* 86:1408–1419.
61. Braun, J., P.S. Hochman, and E.R. Unanue. 1982. Ligand-induced association of surface immunoglobulin with the detergent-insoluble cytoskeletal matrix of the B lymphocyte. *J. Immunol.* 128:1198–1204.
62. Naqvi, S.N., R. Zahn, D.A. Mitchell, B.J. Stevenson, and A.L. Mun. 1998. The WASp homologue Las17p functions with the WIP homologue End5p/verprolin and is essential for endocytosis in yeast. *Curr. Biol.* 8:959–962.
63. Fischer, K.D., A. Zmuldzinas, S. Gardner, M. Barbacid, A. Bernstein, and C. Guidos. 1995. Defective T-cell receptor signalling and positive selection of Vav-deficient CD4+ CD8+ thymocytes. *Nature.* 374:474–477.
64. Tarakhovsky, A., M. Turner, S. Schaal, P.J. Mee, L.P. Duddy, K. Rajewsky, and V.L.J. Tybulewicz. 1995. Defective antigen receptor-mediated proliferation of B and T cells in the absence of Vav. *Nature.* 374:467–470.
65. Zhang, R., F.W. Alt, L. Davidson, S.H. Orkin, and W. Swat. 1995. Defective signaling through T- and B-cell antigen receptors in lymphoid cells lacking the Vav proto-oncogene. *Nature.* 374:470–473.
66. Crespo, P., K.E. Schuebel, A.A. Ostrom, J.S. Gutkind, and X.R. Bustelo. 1997. Phosphotyrosine-dependent activation of Rac-1 GDP/GTP exchange by the Vav proto-oncogene product. *Nature.* 385:169–172.
67. Han, J.W., B. Das, W. Wei, L. Van Aelst, R.D. Mosteller, R. Khosravi-Far, J.K. Westwick, C.J. Der, and D. Broek. 1997. Lck regulates Vav activation of members of the Rho-family of GTPases. *Mol. Cell Biol.* 17:1346–1353.
68. Dustin, M.L., M.W. Olszowy, A.D. Holdorf, J. Li, S. Bromley, N. Desai, P. Widder, F. Rosenberger, P.A. van der Merwe, P.M. Allen, and A.S. Shaw. 1998. A novel adaptor protein orchestrates receptor patterning and cytoskeletal polarity in T-cell contacts. *Cell.* 94:667–677.
69. Wülfing, C., and M.M. Davis. 1998. A receptor/cytoskeletal movement triggered by costimulation during T cell activation. *Science*. 282:2266–2269.
70. Valitutti, S., M. Dessing, K. Aktories, H. Gallati, and A. Lanzavecchia. 1995. Sustained signaling leading to T cell activation results from prolonged T cell receptor occupancy. Role of T cell actin cytoskeleton. *J. Exp. Med.* 181:577–589.
71. Wülfing, C., M.D. Sjaastad, and M.M. Davis. 1998. Visualizing the dynamics of T cell activation: intracellular adhesion molecule 1 migrates rapidly to the T cell/B cell interface and acts to sustain calcium levels. *Proc. Natl. Acad. Sci. USA*. 95: 6302–6307.